



Article

Biological and Geochemical Development of Placer Gold Deposits at Rich Hill, Arizona, USA

Erik B. Melchiorre ^{1,2,*} , Paul M. Orwin ³, Frank Reith ^{4,5}, Maria Angelica D. Rea ^{4,5} , Jeff Yahn ⁶ and Robert Allison ⁷

¹ Department of Geology, California State University, 5500 University Parkway, San Bernardino, CA 92407, USA

² Department of Earth Sciences, University of California Riverside, 900 University Avenue, Riverside, CA 92521, USA

³ Department of Biology, California State University, 5500 University Parkway, San Bernardino, CA 92407, USA; porwin@csusb.edu

⁴ Department of Molecular and Cellular Biology, School of Biological Sciences, The University of Adelaide, Adelaide, South Australia 5005, Australia; frank.reith@csiro.au (F.R.); angel.rea@adelaide.edu.au (M.A.D.R.)

⁵ CSIRO Land and Water, Environmental Contaminant Mitigation and Technologies, PMB2, Glen Osmond, South Australia 5064, Australia

⁶ J.W. Mining, Wickenburg, AZ 85390, USA

⁷ Rob's Detectors, Surprise, AZ 85374, USA

* Correspondence: emelch@csusb.edu; Tel.: +1-909-537-7745

Received: 18 January 2018; Accepted: 5 February 2018; Published: 8 February 2018

Abstract: Placer gold from the Devils Nest deposits at Rich Hill, Arizona, USA, was studied using a range of micro-analytical and microbiological techniques to assess if differences in (paleo)-environmental conditions of three stratigraphically-adjacent placer units are recorded by the gold particles themselves. High-angle basin and range faulting at 5–17 Ma produced a shallow basin that preserved three placer units. The stratigraphically-oldest unit is thin gold-rich gravel within bedrock gravity traps, hosting elongated and flattened placer gold particles coated with manganese-, iron-, barium- (Mn-Fe-Ba) oxide crusts. These crusts host abundant nano-particulate and microcrystalline secondary gold, as well as thick biomats. Gold surfaces display unusual plumate-dendritic structures of putative secondary gold. A new micro-aerophilic Betaproteobacterium, identified as a strain of *Comamonas testosteroni*, was isolated from these biomats. Significantly, this “black” placer gold is the radiogenically youngest of the gold from the three placer units. The middle unit has well-rounded gold nuggets with deep chemical weathering rims, which likely recorded chemical weathering during a wetter period in Arizona’s history. Biomats, nano-particulate gold and secondary gold growths were not observed here. The uppermost unit is a pulse placer deposited by debris flows during a recent drier period. Deep cracks and pits in the rough and angular gold from this unit host biomats and nano-particulate gold. During this late arid period, and continuing to the present, microbial communities established within the wet, oxygen-poor bedrock traps of the lowermost placer unit, which resulted in biological modification of placer gold chemistry, and production of Mn-Fe-Ba oxide biomats, which have coated and cemented both gold and sediments. Similarly, deep cracks and pits in gold from the uppermost unit provided a moist and sheltered micro-environment for additional gold-tolerant biological communities. In conclusion, placer gold from the Devils Nest deposits at Rich Hill, Arizona, USA, preserves a detailed record of physical, chemical and biological modifications.

Keywords: gold; placer; nano-particulate; biomat; *Comamonas testosteroni*; Arizona

1. Introduction

The occurrence of natural gold alloys of $\text{Au} + \text{Ag} \pm \text{Cu}$ (hereafter referred to as native primary gold) within lode ore deposits is well understood and has long been interpreted as having a shallow hydrothermal origin ([1,2] and the references there in). Placer gold occurrence has been attributed to primary, secondary and a combination of primary and secondary formation [3]. In the most established theory of primary placer formation, a gold mass forms as a lode deposit during a hydrothermal event and survives physical and chemical weathering as native gold grains due to the low chemical reactivity and malleability of gold [1,4]. However, a secondary, accretionary origin for some placer gold has been suggested by observations of bacterioform gold, high-purity gold overgrowths and nanoparticulate gold in biomats [3,5–9]. Other authors have rejected low-temperature or biogeochemical nugget growth and suggested an abiological, high-temperature origin within lode deposits [10]. The recent consensus of many workers is that the processes of both primary and secondary models likely play a role in placer gold formation, with the specific contribution of each end member varying from location to location [3,11–13].

Native gold is usually alloyed with traces of lead [14,15], permitting measurement of the lead isotope signal to provide insights into potential source(s) and process(s) that contributed to placer formation [16–18]. The placer gold from the Rich Hill District of Arizona has Pb isotopic signatures distinct from local lode sources, with gold from two of the placer units containing far more radiogenic Pb than the inferred lode source [16]. Those authors concluded that the most plausible scenario to explain the lead isotope signature of placer gold from Rich Hill is the addition of appreciable amounts of secondary gold within the placer environment by geochemical or biological processes [16]. Further work on placer gold from the Rich Hill District of Arizona found that the geochemical and morphological characteristics of the gold provided insights on the lode origins, weathering history and transport history of the placer gold contained within the distinct placer units at this locality [18]. In the present study, we examine the role that microbial activity plays in the formation and modification of placer gold at distinct times during the evolution of the three main placer units of the Devils Nest area at Rich Hill: the red, white and black placers.

2. History and Geological Setting

The Rich Hill District of Arizona (also known as the Weaver II District) is located in the Transition Zone of central Arizona, USA (Figure 1). Official placer gold production, from the discovery in 1863 to present, is 100,000 troy ounces (3110 kg). However, the real total production is likely much higher as considerable amounts of gold likely went unreported in this remote district [19–22]. This district, and especially the Devils Nest area within it, is noted for an abundance of very large, i.e., multi-ounce (>31.1 g), nuggets (Figure 2). The Devils Nest was named by early miners for the abundance of >1-m boulders within the upper reddish sediments of the placers, which greatly hindered early human-powered placer mining operations. Modern placer operations by J.W. Mining and others have yielded hundreds of troy ounces of gold, including over 100 nuggets >1 troy ounce (>31.1 g) (Figure 2), with one confirmed nugget recovered in 2010 weighing 19 troy ounces (591 g). Known lode gold sources of placers at Rich Hill are dominated by the Octave-Beehive vein (red line, Figure 1). The Octave (including the Joker Shaft) and Beehive Mines along this vein were most active from 1895–1942 and produced a combined minimum of 100,000 troy ounces (3110 kg) of gold [22]. The Meyers and Johnson mines exploit separate lodes, which have produced <25,000 troy ounces (<778 kg) of gold [23].

Rich Hill District bedrock geology consists of metavolcanic and metasedimentary rocks of the 1.74–1.8 Ga Yavapai Supergroup [24,25] and the 1.7–1.75 Ga “Granite of Rich Hill” [26]. The metamorphic and granitic units are cut by diabase dikes, which are mineralogically and chemically similar to the 1.1-Ga diabase veins found in the Sierra Ancha Mountains and other locations throughout central Arizona [27]. The lode gold mineralization in the Rich Hill district must be younger than 1.4 Ga and older than 103.7 Ma based on available data [26].

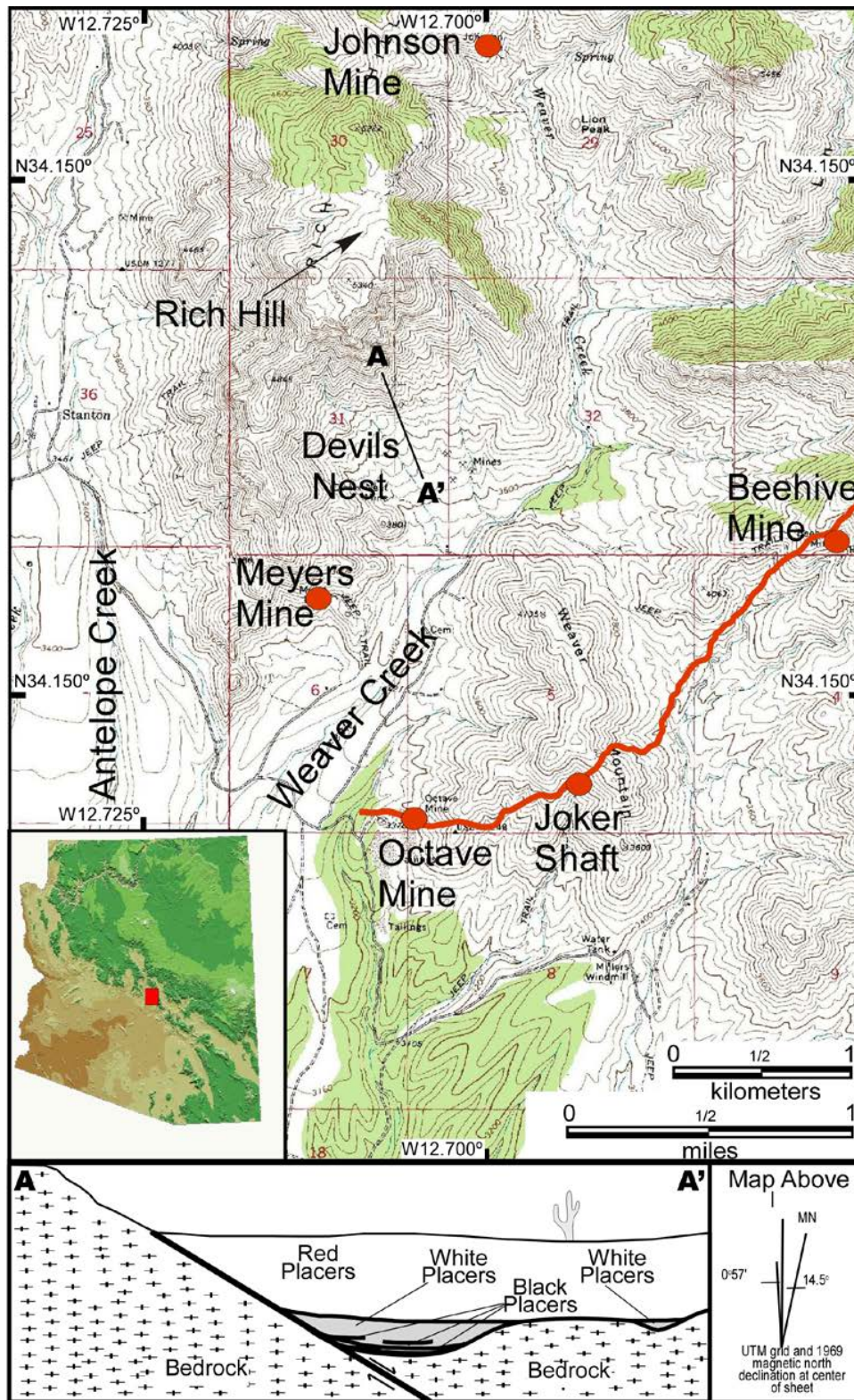


Figure 1. Map of the Rich Hill area; inset showing the location of the district in Arizona (modified from [16]). Dots show the location of major lode gold mines, with the name. The solid red line is the surface trace of the Octave-Beehive vein. The red, white and black placers of the Devils Nest occur within the broad inclined valley on the southeast side of Rich Hill. Cross-section A–A’ shows a schematic view of the different types of placers in the Devils Nest deposit and their relative stratigraphic positions.

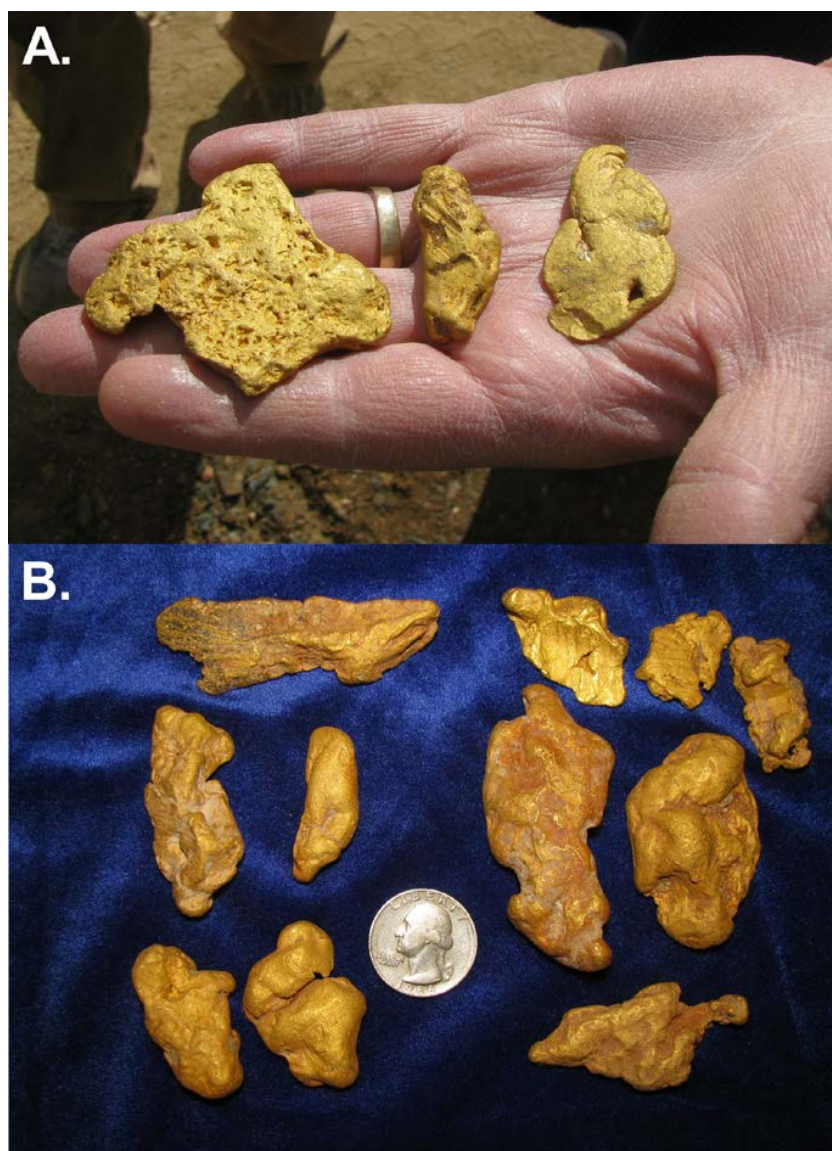


Figure 2. Troy ounce-sized (>31.1 g) gold nuggets from the Devils Nest placer of the Rich Hill area, mined in 2010–2015 by J.W. Mining. These nuggets come from the red, white and black placer deposits, with the majority being found at the base of the red placer.

Lode gold veins contain quartz + pyrite \pm galena \pm chalcopyrite \pm sphalerite, in addition to native gold and electrum [23]. The lode veins range from a few centimeters to two meters in thickness, striking northeast and dipping about 30° to the north. The Octave-Beehive vein is the main lode, and it extends over a distance of about 1.6 km. Native gold in this deposit occurs mainly as microscopic particles and is rarely seen in the lode. Recent work on vein material from the district [16] has shown that gold in the lode mainly occurs as 1–20- μ m inclusions within and coating sulfide minerals, averaging 85 wt % Au and 14 wt % Ag. The paucity of visible native gold within the lode, and the very large size of local placer nuggets, troubled early workers and geologists at the Octave mine [28]. Until modern work identified possible (bio)geochemical mechanisms for large nugget formation in situ [3,29,30], no viable mechanism existed to explain the formation of large nuggets within short distances from a fine-grained gold lode source.

Gold-bearing modern stream sediments, older fluvial placer deposits and gold-bearing debris flow materials occur in an approximately 16-square kilometer area centered on these vein deposits.

Placer gold occurs as traces within the sediments of the modern, active channel of Weaver Creek. Most of the placer gold in the district occurs within older placers of the Devils Nest sequence. The top-most of these units is the “red placers”, which are colored and well-cemented by dried iron-rich red smectite clay, which makes up a large percentage of the matrix of the unit (Figure 3). Red placers are the thickest placer unit, ranging from a few meters to over 15-m thick. Sedimentary clasts are well-rounded to sub-angular, ranging from silt and sand to boulders over one meter diameter shed by local granite and metamorphic rocks. The red placer unit is a series of ancient debris flows and landslides [18]. Gold particles range from 0.1 mm with a mass of a few milligrams to fist-sized nuggets with masses measured in kilograms (Figures 2 and 3).

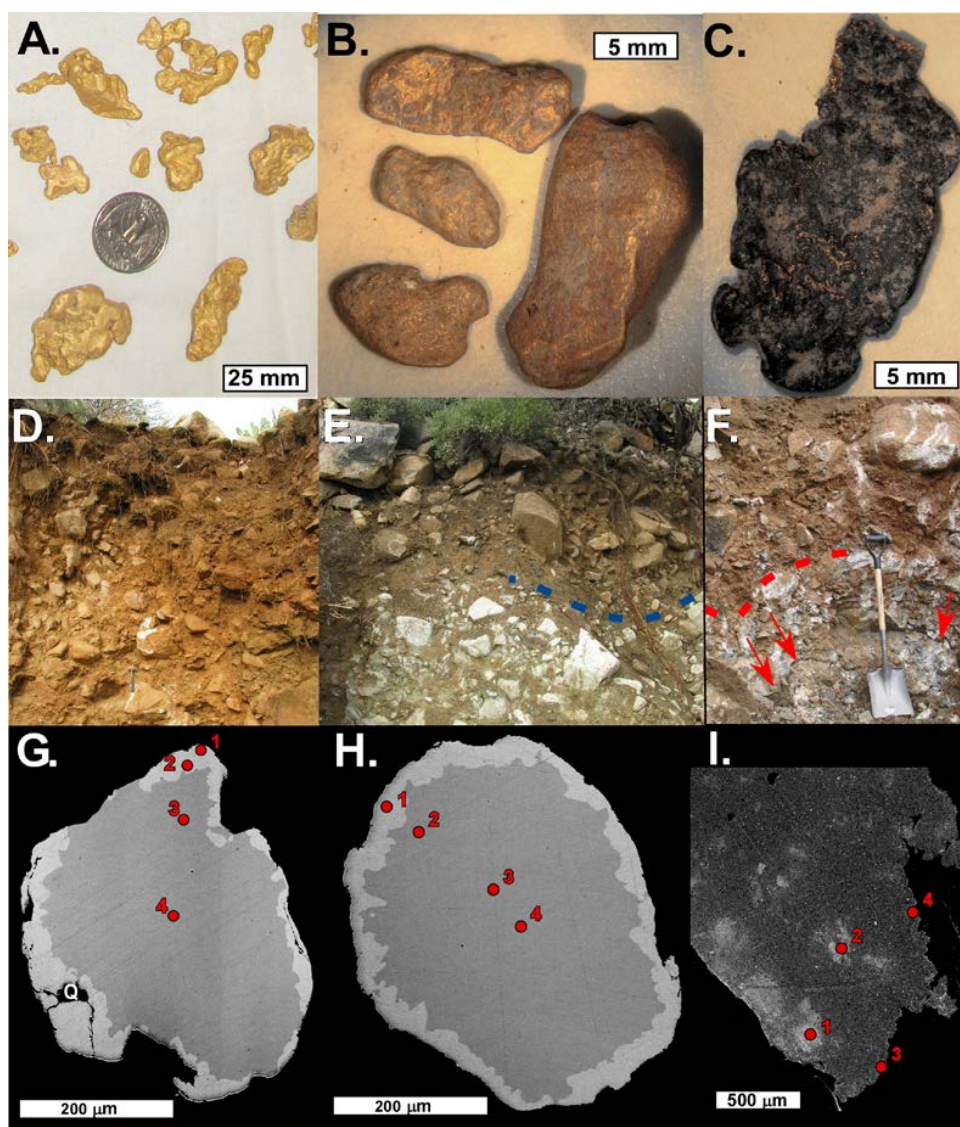


Figure 3. Samples of placer gold from the (A) red placer (B) white placer (C) and black gravel placers, showing representative grain morphologies (after [18]). The placers that contained this gold are also unique in appearance due to (D) iron staining and smectite clay in red placers, (E) bleached cobbles and boulders of bedrock in white placers (dashed line marks boundary between upper modern overburden and lower placer material) (F) and thin black manganese-rich zones above bedrock within local bedrock lows. Enrichment rims are thin and irregular in red placer gold (G), thick and continuous in white placer gold (H) and splotchy and irregular in black placer gold (I). Red dots show electron microprobe (EPMA) probe analysis locations for data presented in Table 1. (G–I) are polished sections.

Table 1. Probe geochemistry of placer gold.

Type	Au (wt %)	Ag (wt %)	Cu (wt %)
Red Placer 1	99.3 ± 0.3	0.62 ± 0.02	0.035 ± 0.003
Red Placer 2	99.5 ± 0.2	0.50 ± 0.02	0.034 ± 0.003
Red Placer 3	90.3 ± 0.2	9.5 ± 0.1	0.044 ± 0.004
Red Placer 4	89.8 ± 0.2	10.1 ± 0.2	0.042 ± 0.003
White Placer 1	99.5 ± 0.2	0.48 ± 0.03	0.029 ± 0.003
White Placer 2	97.5 ± 0.1	2.4 ± 0.2	0.031 ± 0.003
White Placer 3	90.4 ± 0.1	9.6 ± 0.1	0.033 ± 0.003
White Placer 4	90.1 ± 0.2	9.8 ± 0.1	0.034 ± 0.003
Black Placer 1	99.3 ± 0.2	0.5 ± 0.8	0.051 ± 0.005
Black Placer 2	99.1 ± 0.1	0.62 ± 0.08	0.052 ± 0.005
Black Placer 3	90.0 ± 0.3	8.7 ± 0.6	0.049 ± 0.003
Black Placer 4	90.2 ± 0.1	8.8 ± 0.7	0.043 ± 0.004

The underlying “white placer” deposit (Figure 3) is typically 1–3 m thick. This deposit consists of much more rounded gold particles than those found in the overlying red placers (Figure 3). Gold particles range from 1 mm with a mass of a few 10s of milligrams, to rounded masses over one troy ounce (>31.1 g). The study of this unit by Scanning Electron Microscope (SEM) and energy dispersive spectrometry analysis (EDS) has revealed that the white appearance is due to bleached cobbles and sediments that are cemented by sericite and highly silicified material [16].

Beneath the white placers, within deep bedrock declivities and as seams <1 m thick near bedrock are thin gold-bearing gravels cemented by black manganese-iron oxides (janggunitite) and barium-manganese oxides (hollandite) [16]. These “black placer” deposits contain elongated, but flattened gold particles encapsulated by manganese-iron oxides up to 80 µm thick (Figure 3). The black gravels are nearly always damp when exposed and have a distinctive musty smell. A lead isotope study of the black gold suggests that this is the most radiogenic of the gold in the Devils Nest placers [16]. Both the red and black placers have unusual characteristics, which have not been fully addressed by these previous studies. These include high-purity gold rims, Mn mineral coatings and the apparent paradox of the stratigraphically-oldest placer unit containing the youngest gold in the Devils Nest placers. We propose that these characteristics are associated with biogenic processes within these placers.

3. Materials and Methods

This study examines placer gold recovered during fortuitous circumstances created by modern placer mining operations and facilitated by the willingness of several mine owners to permit scientific study of their gold. Fifteen samples were obtained from each of the localities, for a total of 45 samples. This project did not examine Potato Patch gold due to the low number of samples available and the conditions of sample collection, which likely introduced bacteria from human handling of the samples. It was not practical to obtain additional samples for this study due to the elevated price of gold, difficulty in maintaining access to claims and time required for obtaining new samples under sterile conditions. Specific sample localities within claim boundaries are not provided due to security concerns.

Samples of placer gold were recovered from placer deposits by utilizing a Keene Engineering vibrostatic dry washer for smaller pieces (0.1–0.5 g), while larger gold (>0.75 g) was recovered with a MINELAB GP-Extreme metal detector. These placer samples represent individual gold particles and nuggets (nuggets defined as masses weighing >1 g or measuring > 4 mm) recovered by, or in the presence of, one or more of the authors. Samples were not cleaned prior to analysis.

Secondary gold structures and morphologies of placer gold samples were imaged using established methods [31]. Samples were mounted on their flattest side to expose the maximum surface area. A LEO Zeiss 1540XB Field Emission Gun-Scanning Electron Microscope (SEM, Carl Zeiss AG,

Jena, Germany) was used to generate Secondary Electron (SE) and Backscatter Electron (BSE) images using an acceleration voltage of 2 or 15 kV, respectively. Concavities on gold grain surfaces were targeted, as they were regions most likely to contain and preserve bacterioform gold structures.

Additional SEM imaging of the exterior surface of representative gold grains mounted on carbon tape was performed with a Cameca SX-100 (Cameca SAS, Gennevilliers, France) at the University of Arizona. The same instrument was used for electron microprobe (EPMA) probe measurements of gold major and silver minor element abundances, using standard off-peak interference and matrix corrections [32,33]. Some samples were embedded within a low-volatile epoxy and polished to expose grain interiors and potential rim chemistry variations, using sequential grits down to a 0.3-micron diamond abrasive. Great care was taken to minimize sample preparation artifacts such as deposition of polishing debris into fractures or pores, localized smearing, which can obscure internal chemistry or physical features, and cross-contamination [34,35]. The error associated with the in situ EPMA trace element microprobe analyses is less than ± 2 wt %.

Elemental analysis of Mn and Fe on the outer surfaces of gold nuggets was performed using a NITON X-Ray Fluorescence (XRF) instrument (Thermo Fisher Scientific, Waltham, MA, USA). The Cu/Zn Mining Mode was used for each analysis, with a dwell time of 240 s. The instrument Metals Mode was not used as our tests suggested that it has lower reproducibility, higher error and did not test for all of the trace elements anticipated in samples. The instrument was calibrated to certified gold-silver-copper-iron-manganese alloy reference standards, and instrumental error was determined to be less than $\pm 10\%$.

Samples collected for biological work were located by a metal detector and removed with a sterile plastic trowel. Each sample was washed five times on-site with sterile 0.9 wt % NaCl solution and stored in this solution, following the methodology outlined in previous work [3]. However, our methodology differs from that of previous work [3], in that samples were not transported to the laboratory on ice. This was done to maintain ambient conditions similar to those within the placer deposit. In the laboratory, samples were washed in sterile double-deionized water to remove salt and air dried.

Biological samples were extracted from the surface of the gold grains in standard PBS (Phosphate-Buffered Saline) and plated on minimal medium (FW-media, Blue Ash, OH, USA; Leadbetter) under anaerobic conditions (Mitsubishi GasPak). To enrich for metal oxidation, we used filter disks impregnated with 1 M FeSO₄ or 1 M MnSO₄. After passage in enrichment culture, isolated colonies were inoculated into thioglycollate broth (Hardy). Microbial growth was observed in a band just below the surface of the reduced medium. Repeated dilution and passage of this culture was performed in thioglycollate broth at approximately three-month intervals, and DNA was extracted from the culture after four passages. The DNA was purified using the Wizard genomic prep kit (Promega) and amplified for 16s sequencing using the well-characterized Lane-1994 universal primers 27f 5'-AGA GTT TGA TYM TGG CTC AG-3' and 1492r 5'-TAC CTT GTT AYG ACT T-3'. Sequencing was carried out by Retrogen, Inc. (San Diego, CA, USA). Sequences were submitted to GenBank as *Comamonas testosteroni* PGI (Placer Gold Isolate). Micrographs were taken on a CoolSnap FX camera using a Zeiss Axioplan 2 (Carl Zeiss AG, Jena, Germany).

4. Results

The four main methods used to examine the placer gold from the Devils Nest placers of Rich Hill are morphological examination using SEM, chemical characterization of outer surfaces using XRF, chemical characterization of gold grain interiors using electron microprobe (EPMA), as well as biological culturing with subsequent biomolecular sequencing of the isolate.

Results of morphological analyses are presented in Figures 4 and 5. Surface textures varied from deformation, which likely resulted from physical weathering, to a wide range of putative (bio)geochemical forms. Gold from the white placer unit (stratigraphic middle unit) was largely restricted to physical weathering forms, with an appearance similar to water-worn nuggets from the

rivers of some Canadian, California and Alaskan placer districts [4,36]. Gold from the red placers showed impact striations and angular surface forms with deep pockets, which contain mat-like structures with a strong morphological resemblance to bacterial mats [16] (Figure 6). Striation marks were dull and weathered, suggesting prolonged exposure to chemical weathering after they were created. These striations are not shiny and fresh as often observed when damaged during mining by heavy equipment. The black placer unit gold has extensive Mn-oxide crusts, which are replete with a wide range of putative biomorphic forms. Scanning electron microscopy imaging revealed that the black coatings are composed of bacterioform structures and contain an abundance of nano-particulate gold, occurring predominantly as octahedral crystals, thin trigonal platelets and spherical forms (Figure 5a–c).

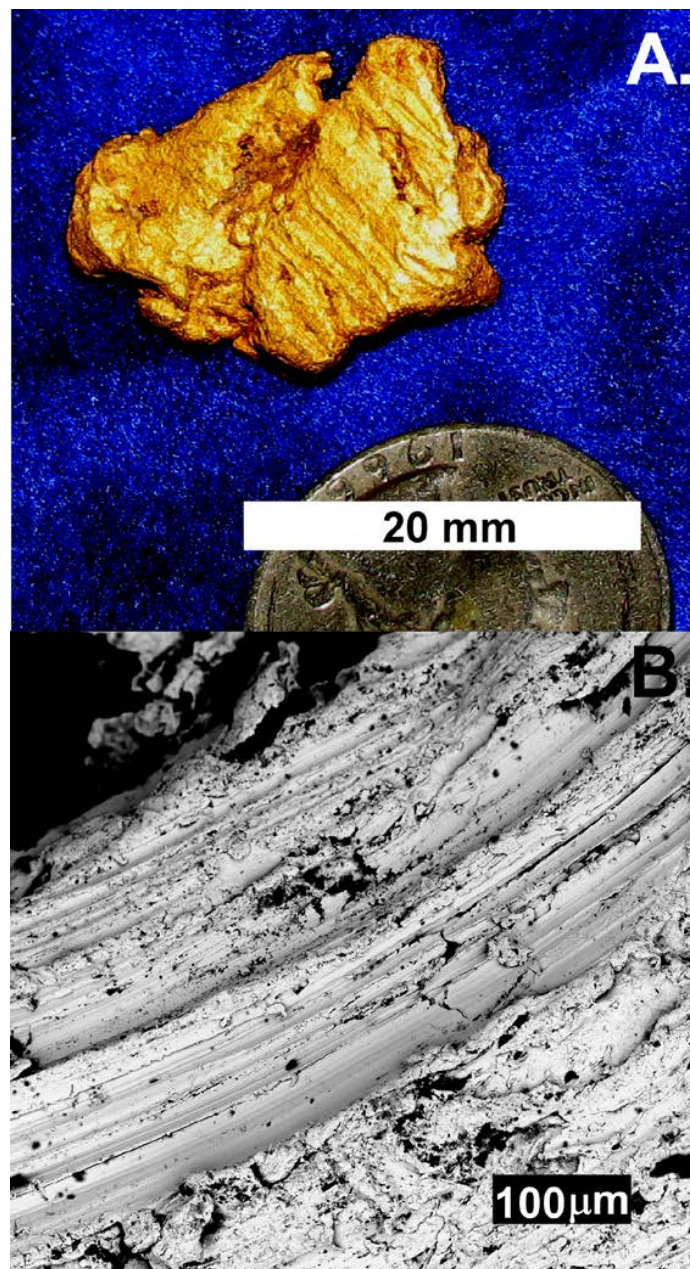


Figure 4. Large nugget with striated surface from transport in traction (A) and SEM image of the detail of the striations (B). Striations are dull, not shiny, like mining-related impact striations.

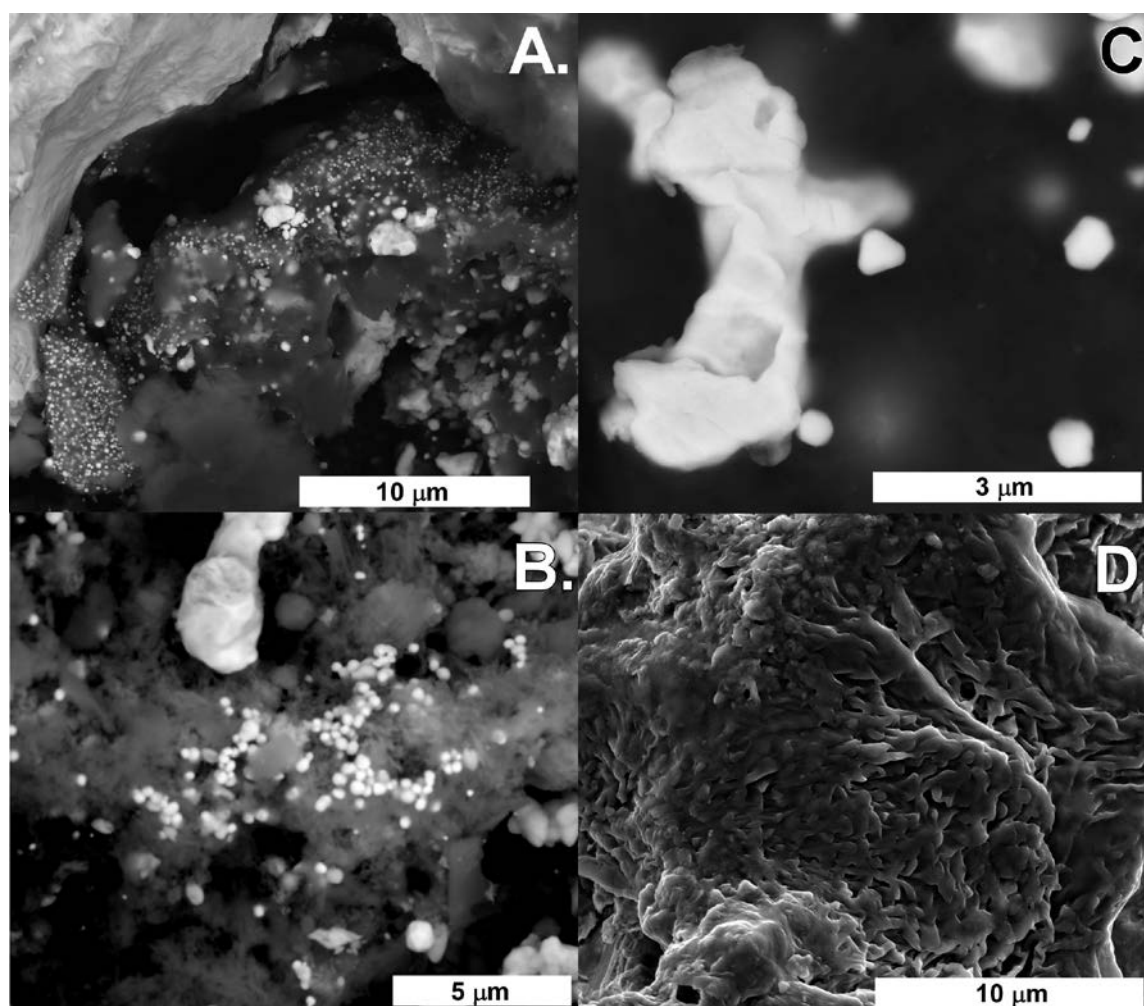


Figure 5. SEM images of black placer gold, showing a pocket of biomats containing abundant nanoparticulate and microcrystalline secondary gold (bright spots) (A). Detail of nanoparticulate gold (bright spots), on grey biomats (B). Detail of nanoparticulate gold (white areas), showing a high degree of crystallinity (C). Underlying Mn-Fe-Ba biocrusts are plumose and dendritic-form gold structures (D).

The XRF characterizations of the surfaces of gold samples are provided in Table 2 and Figure 6. Red placer gold was richer in silver (averaging 11,000 mg/kg) and intermediate in copper and iron (averaging 370 and 38,000 mg/kg, respectively), relative to placer gold from the other units. White placer gold was poorest in trace element concentrations, averaging 3400 mg/kg silver, 310 mg/kg copper and 4700 mg/kg iron. Red and white placer gold had manganese concentrations that were below the limits of detection. Black placer gold is rich in iron and manganese (averaging 52,000 and 4400 mg/kg, respectively) and has the highest copper and lowest silver concentrations (averaging 460 and 1600 mg/kg, respectively). Table 1 and Figure 2 present the results of detailed probe element analysis of placer gold grains in cross-section. Red placer gold has locally well-developed gold-rich rims, which can be absent in some sections of the outer surface. White placer gold typically has well-developed gold-enriched rims that are thick and complete around the entire gold particle. Black placer gold usually has splotchy rims and interior zones of gold enrichment. The enriched zones of the black gold have irregular and diffuse borders, whereas the rims of enrichment on red and white placer gold are sharp and distinct demarcations.

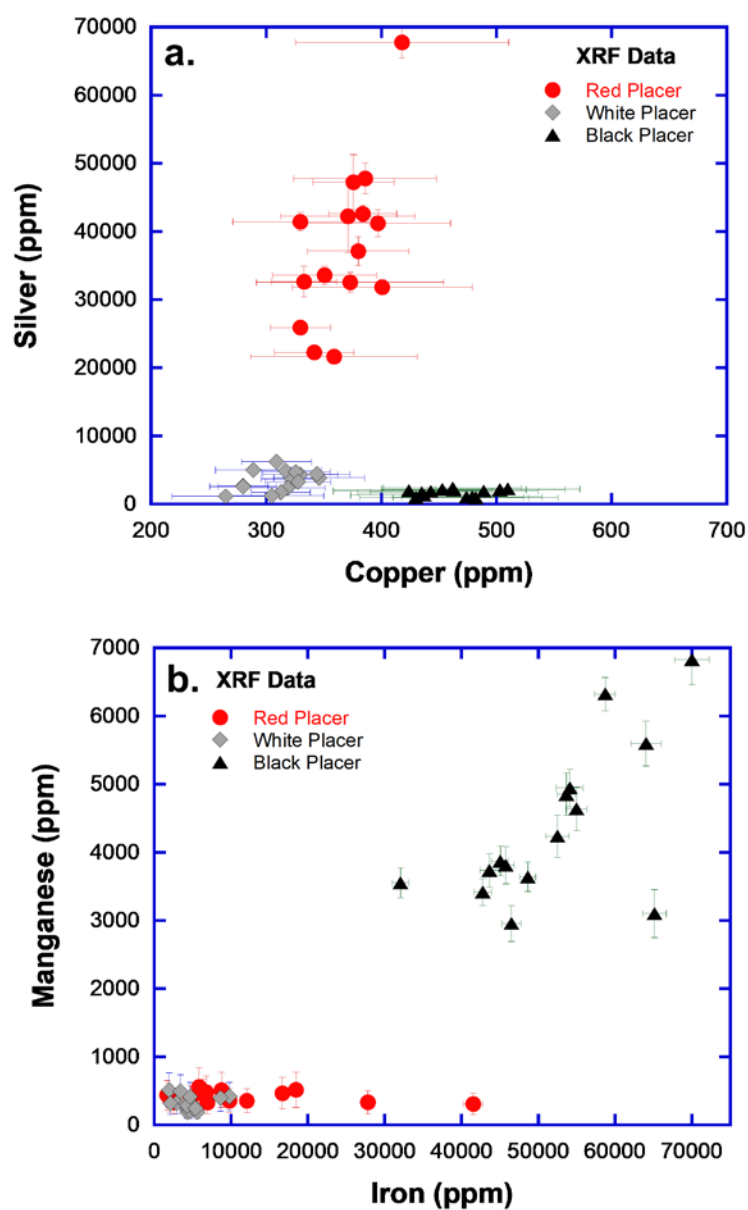


Figure 6. Plot of silver vs. copper (A), and manganese vs. iron (B), as determined by portable XRF analysis for gold particle sample listed in Table 2. Error bars are shown, where larger than symbol size.

Table 2. XRF geochemistry of placer gold.

Sample Number	Type	Au (wt%)	Ag (mg/kg)	Cu (mg/kg)	Mn (mg/kg)	Fe (mg/kg)
JY2	Red Placer	95.3 ± 0.4	47,000 ± 4000	380 ± 40	< LOD	1700 ± 200
JY3	Red Placer	95.1 ± 0.4	48,000 ± 2000	390 ± 60	< LOD	2000 ± 300
JY4	Red Placer	96.7 ± 0.4	33,000 ± 1000	370 ± 80	< LOD	6900 ± 400
JY5	Red Placer	97.6 ± 0.3	21,600 ± 900	360 ± 70	< LOD	5800 ± 300
JY8	Red Placer	95.7 ± 0.1	37,100 ± 2000	380 ± 40	< LOD	18,500 ± 600
JY9	Red Placer	94.4 ± 0.3	43,000 ± 1000	380 ± 30	< LOD	16,700 ± 500
JY11	Red Placer	96.0 ± 0.3	32,000 ± 1000	400 ± 80	< LOD	6400 ± 300
JY12	Red Placer	93.2 ± 0.4	68,000 ± 2000	420 ± 90	< LOD	12,100 ± 400
JY13	Red Placer	97.3 ± 0.3	22,300 ± 900	340 ± 30	< LOD	9800 ± 400
EM1	Red Placer	97.1 ± 0.3	25,900 ± 500	330 ± 30	< LOD	8800 ± 400
EM2	Red Placer	94.8 ± 0.1	42,000 ± 5000	370 ± 60	< LOD	27,900 ± 900
EM3	Red Placer	95.7 ± 0.3	41,000 ± 2000	400 ± 60	< LOD	6800 ± 400

Table 2. Cont.

Sample Number	Type	Au (wt%)	Ag (mg/kg)	Cu (mg/kg)	Mn (mg/kg)	Fe (mg/kg)
EM4	Red Placer	96.6 ± 0.3	34,000 ± 1000	350 ± 50	< LOD	2500 ± 300
EM5	Red Placer	95.6 ± 0.3	41,000 ± 1000	330 ± 60	< LOD	4700 ± 300
EM6	Red Placer	95.8 ± 0.1	32,999 ± 2000	330 ± 30	< LOD	42,000 ± 1300
JY19	White Placer	99.5 ± 0.3	4300 ± 100	330 ± 30	< LOD	2900 ± 700
JY14	White Placer	99.7 ± 0.3	2600 ± 100	280 ± 20	< LOD	4100 ± 300
JY15	White Placer	99.4 ± 0.4	6200 ± 200	310 ± 30	< LOD	1900 ± 200
JY16	White Placer	99.5 ± 0.3	3800 ± 100	350 ± 40	< LOD	9800 ± 400
JY17	White Placer	99.5 ± 0.4	3700 ± 100	320 ± 20	< LOD	2100 ± 600
JY7	White Placer	99.5 ± 0.3	4400 ± 100	340 ± 30	< LOD	8600 ± 400
EM14	White Placer	98.9 ± 0.3	4900 ± 100	320 ± 30	< LOD	4900 ± 300
EM15	White Placer	99.1 ± 0.3	4600 ± 100	330 ± 30	< LOD	4300 ± 200
RA W1	White Placer	99.6 ± 0.2	2300 ± 100	320 ± 30	< LOD	3400 ± 100
RA W2	White Placer	99.6 ± 0.4	1700 ± 40	310 ± 30	< LOD	4300 ± 100
RA W3	White Placer	99.8 ± 0.1	1120 ± 60	270 ± 50	< LOD	4600 ± 100
RA W4	White Placer	99.8 ± 0.2	1220 ± 70	310 ± 50	< LOD	4200 ± 100
RA W5	White Placer	99.4 ± 0.2	3200 ± 100	330 ± 30	< LOD	4700 ± 100
RA W6	White Placer	99.0 ± 0.1	5000 ± 200	290 ± 30	< LOD	5600 ± 100
RA W7	White Placer	99.7 ± 0.4	2600 ± 300	280 ± 20	< LOD	5400 ± 300
JY6	Black Placer	99.8 ± 0.1	1300 ± 100	440 ± 60	3600 ± 20	32,000 ± 1000
JY21	Black Placer	99.9 ± 0.2	970 ± 70	430 ± 50	4900 ± 300	54,000 ± 1700
JY22	Black Placer	99.5 ± 0.3	2140 ± 60	450 ± 50	3900 ± 200	45,000 ± 1000
JY23	Black Placer	98.9 ± 0.5	2300 ± 50	460 ± 60	6800 ± 400	70,000 ± 2200
JY24	Black Placer	99.3 ± 0.3	1630 ± 60	440 ± 60	5600 ± 300	64,000 ± 2000
JY25	Black Placer	99.9 ± 0.2	900 ± 50	480 ± 40	4200 ± 300	53,000 ± 2000
EM10	Black Placer	99.7 ± 0.3	1960 ± 60	420 ± 60	3100 ± 400	65,000 ± 2000
EM11	Black Placer	99.6 ± 0.2	1870 ± 60	490 ± 50	4600 ± 300	55,000 ± 1000
EM12	Black Placer	99.3 ± 0.2	2100 ± 70	500 ± 60	3800 ± 300	46,000 ± 1000
EM 14	Black Placer	99.9 ± 0.3	990 ± 70	470 ± 50	3700 ± 200	44,000 ± 1200
RA B1	Black Placer	99.7 ± 0.2	2210 ± 70	510 ± 60	3000 ± 300	47,000 ± 1000
RA B2	Black Placer	99.8 ± 0.1	920 ± 60	480 ± 70	4900 ± 300	54,000 ± 1000
RA B3	Black Placer	99.7 ± 0.3	2100 ± 80	460 ± 60	3600 ± 200	49,000 ± 1000
RA B4	Black Placer	99.9 ± 0.2	1060 ± 50	480 ± 60	6300 ± 200	59,000 ± 1000
RA B5	Black Placer	99.5 ± 0.2	1800 ± 100	440 ± 50	3400 ± 200	43,000 ± 1000

For microbial growth experiments, the sample from the white placer unit produced no growths during the 18-month period in which it was cultured. The red placer sample produced minor growths, but was insufficient to perform sequencing. However, the gold from the black placers produced abundant growths. Sequencing data of four independent clones identified the isolate as a member of the Betaproteobacteria, with highest identity to an unusual strain within the species *Comamonas testosteroni*.

5. Discussion

5.1. Geochemistry of Rich Hill Placer Gold

The bulk geochemistry and chemical zonation of placer gold can be used to fingerprint the origins of the gold and the conditions of its weathering history [18]. Elemental abundances within the placer gold alloy provide unique identifiers for geochemical classification of placer gold from the Rich Hill district [18]. Non-destructive analysis of Devils Nest placer gold surfaces using XRF can also be used to reliably identify the placer unit of origin [18] (Figure 3a,c). Furthermore, the same authors established that the morphology and chemistry of placer gold from the main placer units at Rich Hill reflect the conditions generated by the past 4–5 Ma of sequential climatic change in Arizona. Gold-rich rims on placer gold are also present, with varying degrees of development and texture, which are distinctive for each of the three placer gold units (Figure 3). The present work expands upon all of the previous studies with new data and provides explanations for the likely origins of these patterns.

5.1.1. Abundances of Silver and Copper

The placer gold from the Devils Nest has silver and copper abundances, as measured by XRF, which are related to the original lode gold source and the development of gold-rich rims. These silver

and copper abundances create fields that are unique for each of the three major placer units (Figure 6a). The red placer unit gold has the highest levels of silver, which is expected with poor development of gold-rich rims and rapid transport within pulse placers. Gold from the white placers is lowest in silver and copper, suggesting deep leaching of these relatively mobile elements. This is consistent with observations in this paper and by others [18] of thick gold-rich rims and a nugget shape, which indicates transport and deposition within an alluvial system during an earlier time (ca. 2.4–3.2 Ma) [18] when Arizona was wetter. Black placer gold is also low in silver, but with intermediate levels of copper and splotchy rim development. This indicates selective addition of high-purity gold and copper. Biogenic and secondary gold deposition is known to generally be of high purity [9,37]. The conditions consistent with biogenic or secondary gold growth are also consistent with conditions of secondary copper mineralization [38,39], which is often associated with manganese known as “copper wad”. Wad ores have long been associated with biogenic origins [40,41]. The black coating on the Devils Nest placer gold at Rich Hill is known to consist of a complex assemblage of manganese-iron-barium oxides [16], and elevated copper is confirmed by this study.

5.1.2. Manganese and Iron Elemental Abundances

Manganese and iron are elements commonly associated with redox chemosynthetic bacteria in the shallow subsurface, particularly within deposits of metals [42–45] and aquifers [46]. Indeed, some are reactive Mn-oxide biominerals (e.g., birnessite), capable of mobilization of gold by oxidizing Au(0) and Au(I) to Au(III) complexes, thereby driving the transformation of gold nuggets [47,48]. Both manganese and iron occur at elevated levels in the coating of the highly transformed black placer gold (Figure 6b), while iron is much lower and manganese very low for the red placer gold. For white placer gold, iron and manganese are both very low. Iron is common in the lode and sediments at Rich Hill, yet manganese minerals are not present in any of the lode sources. The low levels of geochemically-available manganese suggest that localized extreme enrichment of manganese occurred within the black placers. Black placer gold also contains much more iron than red or white placers. This is especially interesting for the red placers as the abundance of iron gives them their color, yet appears to impart little iron to the placer gold alloy or coatings.

It is possible that iron and manganese are concentrated within specific stratigraphic horizons due to redox or geochemical zonation within the placers at the Devils Nest. However, there is no geological evidence of this as the geochemistry of the placer gold correlates with stratigraphic position of the gold, regardless of the relative depth and thickness of the placer units. The sole unifying factor appears to be the presence or absence of pore waters trapped by bedrock depressions, with zones of elevated soil moisture correlating with black placer development. The combination of elevated Fe and Mn associated with the gold nuggets from the black placers, and the geological context, suggests a potential biological origin as both elements are known to be intimately involved with and concentrated by chemosynthetic life within the shallow subsurface in the presence of water [45]. The correlation of black gold coatings with modern high soil moisture in bedrock pockets suggests that biogenic processes are currently active and contribute to the transformation of the placer gold.

5.1.3. Rim Enrichments and Elemental Abundances

Silver and copper solubilities are orders of magnitude greater than that of gold [49,50]. Therefore, the alloy in the outer surface of natural gold nuggets should become depleted in silver and copper, relative to the interior of the nugget, over geologic time. This abiological process of “depletion gilding” or recrystallization is suggested by some [10,13,51] to account for the gold-rich rim effects observed in many placer gold districts. Conversely, others suggest that gold-rich rims result from the addition of high-purity gold to the outer surface of gold by geochemical and biological processes [6,9]. Direct resolution of this long-debated issue is not the immediate goal of this paper.

The gold-rich rims on grains and nuggets from the white placers are typical of the rims observed for deeply chemically-weathered placer gold in alluvial environments [4,36,52]. Given the smooth

outer surfaces produced by mechanical weathering in the steep streams of the Devils Nest, and the difficulties this would pose for the establishment of gold-tolerant microbial communities, it is possible that the gold-rich rims are a result of abiological differential chemical weathering of silver and copper. However, the same weathering could have been responsible for erosion and removal of all evidence of such microbial communities if they ever existed.

The red placer gold was transported more recently by debris flows as pulse placers during a period post-2.4 Ma that was drier, relative to present conditions [18]. This rapid transport and deposition permitted preservation of fragile biological mats, which suggests that gold rims were minimally modified by abrasion during transport. The rims on the gold from these red placers are thinner and incomplete in many places, indicating that the conditions that produced the gold rims were in place for less time, or the processes were less vigorous. Both possibilities are simultaneously possible, as rapid transport and an arid climate [18] would minimize the time and fluids that are essential to deep biological or chemical weathering.

The black gold has splotchy and irregular gold-rich rims and regions. Some of these gold-rich regions lie deep within placer gold grains. This likely reflects the zones of porosity, which are observed when great care is taken with both polishing and the removal of the outer black coating. Unlike the red and white placer gold, black gold has its highest copper concentrations (up to 522 mg/kg) in the gold-rich regions. This likely reflects the copper enrichment associated with the formation of the manganese crusts mentioned in Section 4.

5.2. Biology of Rich Hill Placer Gold

It is well-known that biogeochemical processes drive the cycling of lode and placer gold through dissolution and re-precipitation processes within the shallow subsurface environment [31,53], though others have questioned this hypothesis [13]. Laboratory studies show that nanophase gold particles form as colloids and euhedral crystals when bacteria are exposed to mobile gold complexes [54–56]. High-purity secondary gold, biomat structures and nanophase gold are jointly considered indicative of biogeochemical processes playing a significant role in placer development [3,53]. Biological culturing and morphological observations of Rich Hill placer gold suggest similar processes were involved in this district.

5.2.1. Microbial Culturing

Biological culturing of placer gold nuggets was performed on samples from the red, white and black placer units. It was not the aim of our simple culturing experiment to fully characterize the bacterial consortia. Rather, it was to determine the presence or absence of such bacteria for future work and identify if possible the main species present. We then use the morphological characteristics of the bacteria for comparative study of bacterioform structures observed within gold grains and manganese crusts.

In laboratory culture studies with gold from the black placers, abundant bacterial growth was observed. The presence of readily culturable bacteria on the placer gold, in combination with the abundant nanophase gold observed in the biomats on the placer gold, suggests a mechanism for gold cycling and biotransformation driven by resident bacteria. This is in agreement with a range of earlier studies, which showed that nanophase gold is readily biomineralized by a range of bacteria occurring on placer gold particles, when they are exposed to mobile gold complexes [5,11,55]. Sequencing data of four independent clones identified the isolate as a member of the Betaproteobacteria, with highest identity to the genus *Comamonas*. This isolate appears to be an obligate microaerophile, while the other known *Comamonas* species have been identified as obligate aerobes [57]. Based on sequence homology within the 16s rDNA gene, this appears to be an unusual strain within the species *Comamonas testosteroni*. Obligate aerobes rely exclusively on oxidative phosphorylation with O₂ as a terminal electron acceptor for growth, while obligate anaerobes are killed or go dormant when exposed to atmospheric levels of oxygen due to lack of enzymes to detoxify oxygen radicals. Microaerophiles occupy an unusual

niche in their ability to withstand small amounts of oxygen and inability to grow effectively under strongly reducing anoxic conditions. This is consistent with the geological context of these samples, as this new strain of *Comamonas* occurs in black gold placers, which only are found deep under thick red placers within stagnant wet potholes in bedrock that is exposed only by extensive mining operations. *Comamonas* species typically have a non-fermentative chemoorganotrophic metabolism [58].

Furthermore, it would not be unusual to find *Comamonas* bacteria within this type of environment. A close relative of this bacterium, *Delftia acidovorans*, is known to be directly involved in active detoxification and precipitation of gold nanoparticles through extracellular conversion of toxic Au(I/III)-complexes via the metallophore delftibactin (Johnson et al., 2013). The reclassification of *Pseudomonas acidovorans* as members of *Comamonas* occurred in 1987 [57]. Prior to this, *Comamonas terrigena* had been the only species since the genus was named in 1985 [59]. Further study of phenotypic characteristics, chemotaxonomic characteristics and DNA homology eventually resulted in *Comamonas acidovorans*' reclassification as *Delftia acidovorans* [59].

Images of this new *Comamonas* species have a striking similarity to the mineralized bacterial mats observed on the black coatings of black placer gold and within deep cracks of red placer gold (Figure 6 in [16]; Figure 7, this paper). Micrographs from the *Comamonas* laboratory culture (Figure 7a,b) show a strong textural similarity to backscatter electron images of the spongy rims on the outer surfaces of black placer gold (Figure 7c). There is strong correlation between the presence of these biomats and rim regions of thick silver/copper depletion (Figure 7c). Workers have shown that toxicity drives the formation of gold-detoxifying biomats that catalyze the biomineralization of gold [60]. Based on what is known of metabolism in other *Comamonas* species, it is suspected that this association is linked to localized aqueous gold toxicity reduction through excretion, rather than chemosynthetic feeding upon a gold substrate.

5.2.2. Red and Black Placer Biomats and Nanophase Gold

Bacterial mats have been observed within deep cracks of red placer gold (Figure 6 in [16]) and on the black coatings of black placer gold (Figure 5). Both are replete with 0.2–0.9 micron nanophase gold particles (Figure 5a). The nano-particles range from amorphous blebs (Figure 5b) to sharp well-defined crystals and plates (Figure 5c). Varying sizes of this secondary gold suggest that several “episodes” of gold cycling occurred. Similar size variability in gold from Queensland, Australia, was suggested to result from at least five major episodes of biogeochemical dissolution and re-precipitation of gold occurred, spanning up to 58 years in total duration [53].

Beneath the surface coatings of the black gold grains, plumose and dendritic growths are observed (Figure 5d), inducing zones of porosity to the otherwise massive gold. These textures consist of elongate structures of the proper dimensions for bacteria and likely represent solid pseudomorphous overgrowths after their original carbon substrate host, similar to that observed by other studies [5]. Collectively, these structures and the abundant bacterioform nano-gold suggest that biologically-mediated dissolution and re-precipitation processes were significant influences.

The red placer gold was transported by debris flows as pulse placers [18]. Transport-related ductile deformation of placer gold is known to occur in these types of environments due to abiogenic processes [61]. This rapid transport and deposition permitted preservation of many deep cracks, pockets and angular surfaces, which normally would have been abraded away and rounded-off in a fluvial placer system. Biomats are not observed on this gold within deep gouges and striated surfaces, which resulted from transport, but are found within deep older depressions. This indicates that the biomats formed before their final emplacement. Conversely, black placer gold has abundant biomat formation on striated surfaces, which were produced by traction transport, indicating biomat formation after final emplacement.

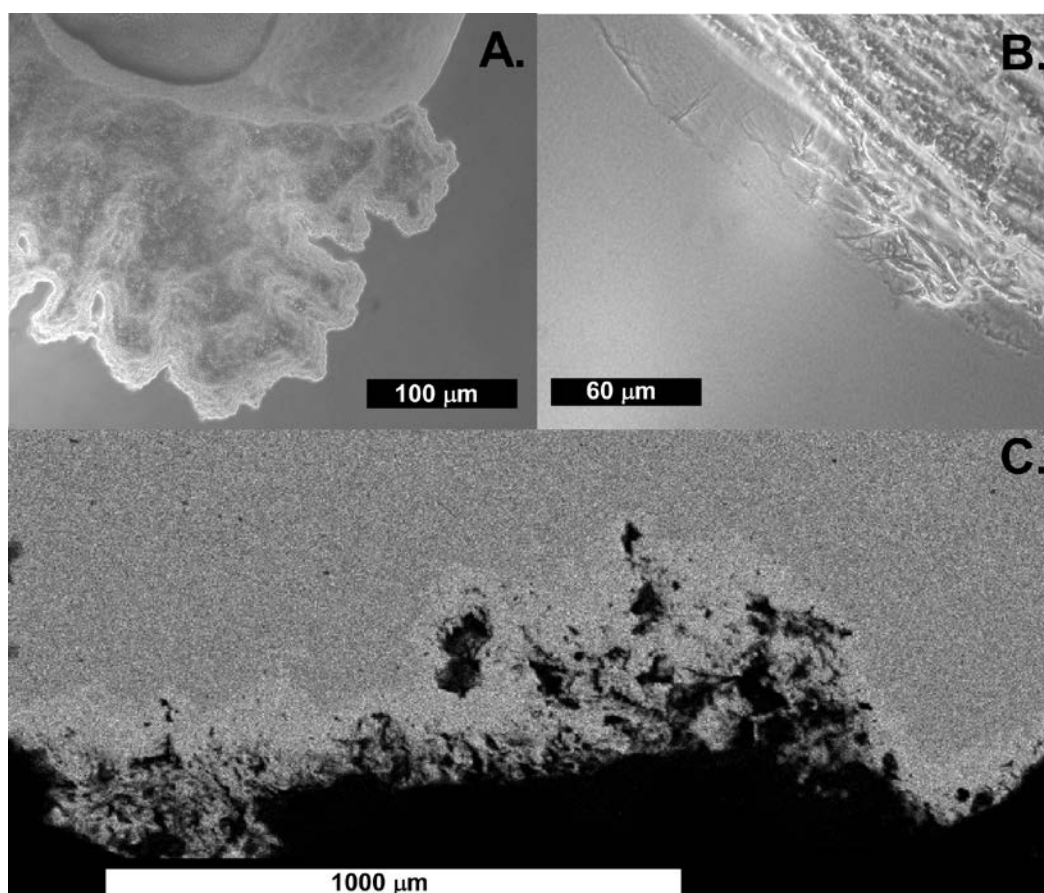


Figure 7. Optical micrographs of (A,B) bacterial growths cultured from biomats growing on black placer gold and (C) backscatter electron image of a biomat zone in cross-section on a small grain of black placer gold. The backscatter image shows zones of deep silver and copper leaching (lighter areas) adjoining the spongy areas of biomat development.

5.3. Origin and Evolution of the Placer Gold Deposits

A feature of Rich Hill placer gold from the red and black Devils Nest deposits is a distinct Pb isotope signal, which is very different from local lode gold. In fact, this gold is more radiogenic than its inferred lode source, which dates to ca. 1580 Ma, suggesting a more recent growth or modification of the nuggets within the placer environment [16,18]. The black placer gold is the most radiogenic, despite its position at the bottom of the placer deposit stratigraphy, suggesting that it is the youngest gold. There is no physical evidence that this black gold has migrated to its present lower position through density settling. The isotope signal is not modern contamination to the outer surface of the gold, or embedded within the black coating, as this gold was micro-abraded to retain only the innermost cores of the nuggets that were analyzed [16]. Based on the association of biomorphic forms, nano-particulate gold and active bacterial growths, we suggest that biomineralization has significantly modified this stratigraphically older gold with a younger Pb isotope overprint. Active in situ growth may even continue to the present day, as the placer gold from this unit has mineralized biomats containing a live *Comamonas* strain.

This would not be unexpected, as the black placers occur in bedrock potholes and low spots that are observed to trap stagnant, oxygen-poor water. Such conditions would produce a different weathering environment than experienced by the red and white placers. The high surface to volume ratio for this flat gold, produced by transport in traction, would facilitate modification of grain cores.

The gold from the white placers is the least radiogenic and therefore least likely to have acquired significant amounts of more recent biogenic gold. It is probable that the deep gold-rich rims on this gold result from chemical weathering. The white placer deposits formed during a period that was wetter and dominated by fluvial systems based on sedimentological evidence and gold particle shape analysis [18]. The smooth and highly rounded gold particle shape was most likely produced by physical weathering in these fluvial systems and would have been conducive to the deep chemical weathering recorded by the silver-copper-depleted alloy of the nugget rims.

An intriguing aspect of the white placers is that the mineralogy of the sediments hosting the gold may be interpreted as part of a fossil low-temperature (<200 °C) hydrothermal system. Weak to moderate silicification and sericitation (boulder bleaching) of these sediments suggest the emergence of a hot spring system within the placer unit. Similar low temperature hydrothermal alteration of a placer unit has been noted for the White Channel sediments of the Klondike District in Canada [62–64]. At Rich Hill, it is possible that in addition to causing the observed quartz-sericite alteration, the chemically- and thermally-aggressive fluids of such a system could have modified pre-existing placer gold nuggets to produce smoother and rounder forms and the deep silver and copper depletion rims. These fluids may have also inhibited biological growth on the gold, through thermal and chemical sterilization.

The red unit is the stratigraphically youngest of the Devils Nest placers, and this gold was deposited during a drier period marked by large seasonal debris flows. As a result of this rapid transport, the gold of the red placers is relatively rough, preserving features from its original lode source and displaying minimal rim effects produced by chemical weathering. The presence of biomats within deeper crevices and pits on the red placer gold, but not on the youngest grooves from transport, and in uniform coatings on the black placer gold suggest contemporaneous timing of biological colonization and modification very late in the development of placers at Rich Hill.

As climate shifted from wet to dry around 1.6 Ma ago [65], soil microbes such as *Comamonas* faced a challenge to adapt to the new climate. Perhaps it was a tolerance to generally toxic aqueous gold, or the high density of gold that provides a thermal impetus for condensation of water, or a combination of these factors that created a localized microclimate suitable for survival. As drying continued, the microbial life retreated to deep cracks, which were able to retain more moisture through surface tension, and deep bedrock pools that had minimal water loss. With smooth surfaces, the gold of the white placers could not readily sustain microbial life. The obligate microaerophile *Comamonas* species was apparently able to make a living within the deep, stagnant and localized black placer environment. At some fairly recent point, the modern braided drainage network began to erode the pre-existing Devils Nest placers, creating a modern alluvial placer deposit with its own distinctive characteristics. Because culture-based analysis necessarily places limitations on microbial growth and it is commonly observed that environmental samples contain many more organisms than can be cultivated, we should be careful to allow for the possibility of many other microbial inhabitants of these putative biomats that remain uncultured. Environmental DNA analysis may shed further light on this microbial habitat.

6. Conclusions

Following 5–17 Ma of high-angle basin and range faulting, a shallow basin was produced on the shoulder of Rich Hill that preserves the three placer gold deposits of the Devils Nest. Gold from these deposits records physical, chemical and biological modification triggered by a wet/dry paleoclimate transition. The lowermost of these units, the black placers, is a thin gold-rich gravel that occurs within bedrock gravity traps, suggestive of a steep gradient and abundant non-seasonal precipitation. Elongated forms suggest gold particle transport was under traction conditions for this radiogenically young gold. The middle unit, the white placers, has well-rounded gold nuggets with deep chemical weathering that also records high levels of non-seasonal precipitation, but with a less steep gradient and abundant fluvial sediment deposition. The uppermost unit, the red placers, was

deposited by a series of landslides and debris flows during a drier period with seasonal precipitation, following the 1.6-Ma [65] wet/dry transition. During this dry period, and continuing to the present, microbial communities established within the wet, oxygen-poor bedrock traps of the lowermost placer unit, and occasionally within deep crevices on gold of the red placers. This resulted in biological modification of placer gold chemistry, the generation of nanoparticulate gold and the production of Mn-Fe-Ba oxide biomats. The young Pb isotope ages for nuggets from these placers indicate the formation or modification of the gold nuggets during recent supergene processes [16]. A new strain of the Betaproteobacterium *Comamonas testosteroni* was cultured from these biomats on the placer gold and was likely involved in the nugget growth by the formation of Au-detoxifying biomats or by serving as a reducing agent. It is likely that the white placer gold was not colonized and biologically modified, due to an unfavorable combination of smooth surfaces, dry conditions and/or low temperature hydrothermal bleaching.

Acknowledgments: Instrumentation was provided and supported by the National Science Foundation, EAR-0115884 and EAR-0941106. XRF instrumentation was provided by a grant from the W.M. Keck Foundation. Support was also provided by a NASA Astrobiology Institute Minority Institution Research Sabbatical (NAI-MIRS) program award to the lead author and an institutional grant by California State University, San Bernardino. The lead author also thanks his colleagues of the Minority Institution Astrobiology Collaborative (MiAC) for providing the supportive environment that made this work possible. CSUSB provided internal funding to support undergraduate participation in this research activity. We thank Ken Domanik at University of Arizona for help with SEM imaging and probe analyses. Lastly, we thank Ed DeWitt for his many hours of guidance over the past decade, prior to his passing in 2013.

Author Contributions: Erik Melchiorre and Paul Orwin conceived and designed the experiments; Paul Orwin and Erik Melchiorre performed the experimental work; Frank Reith, Maria Angelica Rea and Erik Melchiorre performed imaging and analyses; Jeff Yahn and Robert Allison contributed materials and provided valuable geological data; Erik Melchiorre wrote the paper, with input from the other authors.

Conflicts of Interest: The authors declare no conflict of interest.

References

- Boyle, R.W. *The Geochemistry of Gold and Its Deposits: Together with a Chapter on Geochemical Prospecting for the Element*; Geological Survey of Canada: Ottawa, ON, Canada, 1979.
- Saunders, J.A.; Unger, D.L.; Kamenov, G.D.; Fayek, M.; Hames, W.E.; Utterback, W.C. Genesis of Middle Miocene Yellowstone-hotspot-related bonanza epithermal Au-Ag deposits, Northern Great Basin, USA. *Min. Depos.* **2008**, *43*, 715–734. [[CrossRef](#)]
- Reith, F.; Fairbrother, L.; Nolze, G.; Wilhelmi, O.; Clode, P.L.; Gregg, A.; Parsons, J.E.; Wakelin, S.A.; Pring, A.; Hough, R.; et al. Nanoparticle factories: Biofilms hold key to gold dispersion and nugget formation. *Geology* **2010**, *38*, 843–846. [[CrossRef](#)]
- Lindgren, W. *Tertiary Gravels of the Sierra Nevada of California*; Professional Paper 78; US Geological Survey: Washington, DC, USA, 1911.
- Watterson, J.R. Artifacts resembling budding bacteria produced in placer-gold amalgams by nitric acid leaching. *Geology* **1994**, *20*, 1144–1146. [[CrossRef](#)]
- Mossman, D.J.; Reimer, T.; Durstling, H. Microbial processes in gold migration and deposition: Modern analogues to ancient deposits. *Geosci. Can.* **1999**, *26*, 131–140.
- Reith, F.; Lengke, M.F.; Falconer, D.; Craw, D.; Southam, G. Winogradski Review: The geomicrobiology of gold. *Int. Soc. Microb. Ecol. J.* **2007**, *1*, 567–584. [[CrossRef](#)]
- Hough, R.M.; Butt, C.R.M.; Fisher-Buhner, J. The crystallography, metallography and composition of gold. *Elements* **2009**, *5*, 297–302. [[CrossRef](#)]
- Southam, G.; Lengke, M.F.; Fairbrother, L.; Reith, F. The biogeochemistry of gold. *Elements* **2009**, *5*, 303–307. [[CrossRef](#)]
- Hough, R.M.; Butt, C.R.M.; Reddy, S.M.; Verrall, M. Gold nuggets: Supergene or hypogene? *Austr. J. Earth Sci.* **2007**, *54*, 959–964. [[CrossRef](#)]
- Fairbrother, L.; Brugger, J.; Shapter, J.; Laird, J.; Southam, G.; Reith, F. Supergene gold transformation: Biogenic secondary and nano-particulate gold from arid Australia. *Chem. Geol.* **2012**, *320*, 17–31. [[CrossRef](#)]

12. Craw, D.; Lilly, K. Gold nugget morphology and geochemical environments of nugget formation, southern New Zealand. *Ore Geol. Rev.* **2016**, *79*, 301–315. [[CrossRef](#)]
13. Stewart, J.; Kerr, G.; Prior, D.; Halfpenny, A.; Pearce, M.; Hough, R.; Craw, D. Low temperature recrystallisation of alluvial gold in paleoplacer deposits. *Ore Geol. Rev.* **2017**, *88*, 43–56. [[CrossRef](#)]
14. Pettke, T.; Frei, R. Isotope systematics in vein gold from Brusson, Val d’Ayas (NW Italy), Pb/Pb evidence for a Piemonte metaophiolite Au source. *Chem. Geol.* **1996**, *127*, 111–124. [[CrossRef](#)]
15. Kamenov, G.D.; Saunders, J.A.; Hames, W.E. Mafic magmas as sources for gold in middle-miocene epithermal deposits of northern Great Basin, USA: Evidence from Pb isotopic compositions of native gold. *Econ. Geol.* **2007**, *102*, 1191–1195. [[CrossRef](#)]
16. Kamenov, G.D.; Melchiorre, E.B.; Ricker, F.N.; DeWitt, E. Insights from Pb isotopes for native gold formation during hypogene and supergene processes at Rich Hill, Arizona. *Econ. Geol.* **2013**, *108*, 1577–1589. [[CrossRef](#)]
17. Standish, C.D.; Dhuime, B.; Chapman, R.J.; Hawkesworth, C.J.; Pike, A.W.G. The genesis of gold mineralisation hosted by orogenic belts: A lead isotope investigation of Irish gold deposits. *Chem. Geol.* **2014**, *378*, 40–51. [[CrossRef](#)]
18. Melchiorre, E.B.; Kamenov, G.D.; Sheets-Harris, C.; Andronikov, A.; Leatham, W.B.; Yahn, J.; Lauretta, D.S. Climate-induced geochemical and morphological evolution of placer gold deposits at Rich Hill, Arizona, USA. *Geol. Soc. Am. Bull.* **2017**, *129*, 193–202. [[CrossRef](#)]
19. Blake, W.P. Report of the Territorial Geologist. In *Report of the Governor of Arizona for 1899*; Arizona Territorial Government: Phoenix, AZ, USA, 1899; pp. 42–153.
20. Tenney, J.B. *Unpublished Field Notes*; Arizona Bureau of Mines and Mineral Technology: Tucson, AZ, USA, 1933.
21. Hall, E.R. Rich Hill Gold Report. In *Arizona Gold Placers and Placering*; Arizona Bureau of Mines and Mineral Technology: Tucson, AZ, USA, 1934; pp. 43–46.
22. Wilson, E.D. *Arizona Gold Placers and Placering*, 5th ed.; Arizona, Arizona Bureau of Mines and Mineral Technology: Tucson, AZ, USA, 1952; pp. 43–46.
23. Metzger, O.H. *Gold Mining and Milling in the Wickenburg Area, Maricopa and Yavapai Counties, Arizona*; U.S. Bureau of Mines Information Circular 6991; U.S. Bureau of Mines: Washington, DC, USA, 1938.
24. Anderson, P. *Stratigraphic Framework, Volcanic-Plutonic Evolution, and Vertical Deformation of the Proterozoic Volcanic belts of Central Arizona*; Jenney, J.P., Reynolds, S.J., Eds.; Geologic Evolution of Arizona: Tucson, AZ, USA, 1989; pp. 57–147.
25. Karlstrom, K.; Ahall, K.I.; Williams, M.L.; McLelland, J.; Geissman, J.W. Long-lived (1.8 to 1.0 Ga) convergent orogen in southern Laurentia, its extensions to Australia and Baltica, and implications for refining Rodinia. *J. Precamb. Res.* **2001**, *111*, 5–30. [[CrossRef](#)]
26. DeWitt, E. *Geochemistry and Tectonic Polarity of Early Proterozoic (1700–1750 Ma) Plutonic Rocks, North-Central Arizona*; Jenney, J., Reynolds, S.J., Eds.; Geologic Evolution of Arizona: Tucson, AZ, USA, 1989; pp. 149–163.
27. Wrucke, C.T. *The Middle Proterozoic Apache Group, Troy Quartzite, and Associated Diabase of Arizona*; Jenney, J.P., Reynolds, S.J., Eds.; Geologic Evolution of Arizona: Tucson, AZ, USA, 1989; pp. 239–258.
28. Nevius, J.N. Resuscitation of the Octave Gold Mine. *Min. Sci. Press* **1921**, *123*, 122–124.
29. Shuster, J.; Southam, G. The in-vitro “growth” of gold grains. *Geology* **2015**, *43*, 79–82. [[CrossRef](#)]
30. Rakovan, J.; Lüders, V.; Massanek, A.; Nolze, G. Gold crystals from the Lena Goldfields, Bodaibo Area, Eastern Siberia, Russia: Exceptional hopped octahedra and pseudomorphs after pyrite. *Rock. Min.* **2017**, *92*, 16–22. [[CrossRef](#)]
31. Shuster, J. Structural and chemical characterization of placer gold grains: Implications for bacterial contributions to grain formation. *Geomicro. J.* **2015**, *32*, 158–169. [[CrossRef](#)]
32. Armstrong, J.T. *Quantitative Analysis of Silicates and Oxide Minerals: Comparison of Monte-Carlo, ZAF and Phi-Rho-Z Procedures*; Newbury, D.E., Ed.; San Francisco Press: San Francisco, CA, USA, 1988; pp. 239–246.
33. Donovan, J.J.; Snyder, D.A.; Rivers, M.L. An improved interference correction for trace element analysis. In *Proceedings of the Annual Meeting-Electron Microscopy Society of America*; San Francisco Press: San Francisco, CA, USA, 1993; pp. 23–28.
34. Knight, J.B.; McTaggart, K.C. Composition of gold from southwestern British Columbia. *BC Dep. Energy Min. Pet. Res. Geol. Fieldwork* **1988**, *1*, 387–394.
35. Douma, Y.; Knight, J.B. Mounting samples in methylmethacrylate for SEM and EMP analysis: *J. Sed.* **1994**, *A64*, 675–677. [[CrossRef](#)]

36. Knight, J.B.; Mortensen, J.K.; Morison, S.R. The relationship between placer gold shape, rimming and distance of fluvial transport as exemplified by gold from the Klondike, Yukon Territory, Canada. *Econ. Geol.* **1999**, *94*, 635–648. [[CrossRef](#)]
37. Freyssinet, P.; Butt, C.R.M.; Morris, R.C. *Piantone, Ore-Forming Processes Related to Lateritic Weathering*; Hedenquist, J.W., Thomson, J.F.H., Goldfarb, R.J., Richards, J., Eds.; Economic Geology Publishing Company: New Haven, CT, USA, 2005; pp. 681–722, ISBN 978-1-887483-01-8.
38. Melchiorre, E.B.; Criss, R.E.; Rose, T.P. Oxygen and carbon isotope study of natural and synthetic malachite. *Econ. Geol.* **1999**, *94*, 245–259. [[CrossRef](#)]
39. Melchiorre, E.B.; Criss, R.E.; Rose, T.P. Oxygen and carbon isotope study of natural and synthetic azurite. *Econ. Geol.* **2000**, *95*, 621–628. [[CrossRef](#)]
40. Trudinger, P.A. Experimental geomicrobiology in Australia. *Earth Sci. Rev.* **1976**, *12*, 259–278. [[CrossRef](#)]
41. Mohapatra, B.K.; Mishra, S.; Singh, P. Biogenic wad in Iron Ore Group of rocks of Bonai-Keonjhar belt, Orissa. *J. Geol. Soc. India* **2012**, *80*, 89–95. [[CrossRef](#)]
42. Ghiorse, W.C. Biology of iron-and manganese-depositing bacteria. *Ann. Rev. Microbio.* **1984**, *38*, 515–550. [[CrossRef](#)] [[PubMed](#)]
43. Polgari, M.; Okita, P.M.; Hein, J.R. Stable isotope evidence for the origin of the Úrkút manganese ore deposit, Hungary. *J. Sed. Res.* **1991**, *61*, 384–393. [[CrossRef](#)]
44. Thamdrup, B. Bacterial manganese and iron reduction in aquatic sediments. In *Advances in Microbial Ecology*; Springer: New York, NY, USA, 2000; pp. 41–84.
45. Lovley, D. Dissimilatory Fe (III)-and Mn (IV)-reducing prokaryotes. In *The Prokaryotes*; Springer: Berlin/Heidelberg, Germany, 2013; pp. 287–308. [[CrossRef](#)]
46. Weber, K.A.; Spanbauer, T.L.; Wacey, D.; Kilburn, M.R.; Loope, D.B.; Kettler, R.M. Biosignatures link microorganisms to iron mineralization in a paleoaquifer. *Geology* **2012**, *40*, 747–750. [[CrossRef](#)]
47. Ta, C.; Brugger, J.; Pring, A.; Hocking, R.K.; Lenehan, C.E.; Reith, F. Effect of manganese oxide minerals and complexes on gold mobilization and speciation. *Chem. Geol.* **2015**, *407*, 10–20. [[CrossRef](#)]
48. Ta, C.; Reith, F.; Brugger, J.L.; Pring, A.; Lenehan, C.E. Analysis of gold (I/III)-complexes by HPLC-ICP-MS demonstrates gold (III) stability in surface waters. *Enviro. Sci. Technol.* **2014**, *48*, 5737–5744. [[CrossRef](#)] [[PubMed](#)]
49. Clever, H.L.; Johnson, S.A.; Derrick, M.E. The solubility of mercury and some sparingly soluble mercury salts in water and aqueous electrolyte solutions. *J. Phys. Chem. Ref. Data* **1985**, *14*, 631–680. [[CrossRef](#)]
50. Barton, A.F. *CRC Handbook of Solubility Parameters and Other Cohesion Parameters*; CRC Press: Routledge, NJ, USA, 2017; ISBN 9780849301766.
51. Groen, J.C.; Craig, J.R.; Rimstidt, J.D. Gold-rich rim formation on electrum grains in placers. *Can. Min.* **1990**, *28*, 207–228.
52. Desborough, G.A. Silver depletion indicated by microanalysis of gold from placer occurrences, western United States. *Econ. Geol.* **1970**, *65*, 304–311. [[CrossRef](#)]
53. Shuster, J.; Lengke, M.; Márquez-Zavalía, M.F.; Southam, G. Floating gold grains and nanophase particles produced from the biogeochemical weathering of a gold-bearing ore. *Econ. Geol.* **2016**, *111*, 1485–1494. [[CrossRef](#)]
54. Watterson, J.R.; Nishi, J.M.; Botinelly, T. *Evidence That Gold Crystals Can Nucleate on Spores of Bacillus Cereus*; Open-File Report 84-487; US Geological Survey: Washington, DC, USA, 1984.
55. Reith, F.; Etschmann, B.; Grosse, C.; Moors, H.; Benotmane, M.A.; Monsieurs, P.; Grass, G.; Doonan, C.; Vogt, S.; Lai, B.; et al. Mechanisms of gold biomineralization in the bacterium *Cupriavidus metallidurans*. *Proc. Natl. Acad. Sci. USA* **2009**, *106*, 17757–17762. [[CrossRef](#)] [[PubMed](#)]
56. Fairbrother, L.; Etschmann, B.; Brugger, J.; Shapter, J.; Southam, G.; Reith, F. Biomineralization of gold in biofilms of *Cupriavidus metallidurans*. *Enviro. Sci. Technol.* **2013**, *47*, 2628–2635. [[CrossRef](#)] [[PubMed](#)]
57. Tamaoka, J.; Ha, D.M.; Komagata, K. Reclassification of *Pseudomonas acidovorans* den Dooren de Jong 1926 and *Pseudomonas testosteroni* Marcus and Talalay 1956 as *Comamonas acidovorans* comb. nov. and *Comamonas testosteroni* comb. nov., with an emended description of the genus *Comamonas*. *Intern. J. Syst. Bact.* **1987**, *37*, 52–59. [[CrossRef](#)]
58. Willems, A.; DeVos, C. *The Prokaryotes*; Dworkin, M., Falkow, S., Rosenberg, E., Schleifer, K., Stackebrandt, E., Eds.; Springer: New York, NY, USA, 2006; pp. 2583–2590.

59. Gilligan, H.; Lum, G.; Vandamme, P.; Whittier, S. Burkholderia, Stenotrophomonas, Ralstonia, Brevundimonas, Comamonas, Delftia, Pandoraea, and Acidovorax. In *Manual of Clinical Microbiology*; ASM Press: Washington, DC, USA, 2003; pp. 729–748.
60. Kerr, G.; Falconer, D.; Reith, F.; Craw, D. Transport-related mylonitic ductile deformation and shape change of alluvial gold, southern New Zealand. *Sedim. Geol.* **2017**. [[CrossRef](#)]
61. Brugger, J.; Etschmann, B.; Grosse, C.; Plumridge, C.; Kaminski, J.; Paterson, D.; Shar, S.S.; Ta, C.; Howard, D.L.; de Jonge, M.D.; et al. Can biological toxicity drive the contrasting behavior of platinum and gold in surface environments? *Chem. Geol.* **2013**, *343*, 99–110. [[CrossRef](#)]
62. Dufresne, M.B. Origin of Gold in the White Channel Sediments of the Klondike Region, Yukon Territory. Master's Thesis, University of Alberta, Edmonton, AB, Canada, 1986.
63. Dufresne, M.B.; Morison, S.R.; Nesbitt, B.E. Evidence of hydrothermal alteration in White Channel sediments and bedrock of the Klondike area, west-central Yukon. *Yuk. Geol.* **1986**, *1*, 44–49.
64. Tempelman-Kluit, D.J. White Channel Gravel of the Klondike. *Yuk. Exp. Geol.* **1979**, *1980*, 7–31.
65. Smith, G.A. Climatic influences on continental deposition during late-stage filling of an extensional basin, southeastern Arizona. *Geol. Soc. Am. Bull.* **1994**, *106*, 1212–1228. [[CrossRef](#)]



© 2018 by the authors. Licensee MDPI, Basel, Switzerland. This article is an open access article distributed under the terms and conditions of the Creative Commons Attribution (CC BY) license (<http://creativecommons.org/licenses/by/4.0/>).